JOURNAL OF THE STRUCTURAL DIVISION

STIFFNESS METHOD FOR CURVED BOX GIRDERS AT INITIAL STRESS

By Zdeněk P. Bažant,[1] M. ASCE and Mahjoub El Nimeiri[2]

INTRODUCTION

Long-span box girder bridges usually can be approximated, for the purpose of global behavior, as thin-wall beams of closed cross section, undergoing longitudinal warping and transverse distortion. The ordinary differential equations of such beams in terms of the parameters of the assumed basic deformation modes of cross section were derived in the general form by Vlasov (27) and were extended by others (3,10). Analytical solutions of some simple practical cases have been obtained by Dabrowski (10), Wittrick, Hemp, Argyris (19), and Benscoter (6). Křístek (13) has simplified the analytical solution by separating, in accordance with the superposition principle, the analysis of transverse distortion from that of torsion with longitudinal warping. For computer matrix analysis the most versatile and convenient formulation is the finite element stiffness method, which was applied to the problem by Scordelis, et al. (17,24) and others (1,14,15,25). Yet the number of unknowns in this approach is very large because the girder is subdivided in both the longitudinal and the transverse directions.

Therefore, attention also has been focused on the stiffness methods that apply discrete subdivision in only one direction. In the exact plate theory solutions by Jenkins (23) and Goldberg and Levy (Ref. 12, for folded plates), the direct stiffness harmonic analysis by Scordelis, et al. (11), and the finite strip method by Cheung (8) and others (18), the discrete subdivision is introduced within the cross section, while in the longitudinal direction Fourier series expansion is assumed. This formulation allows easy handling of various cross-sectional shapes and is appropriate mainly for relatively short box girders. For long box girders, and especially for multispan beams, a discrete subdivision in the longitudinal (rather than transverse) direction, i.e., a subdivision into beam

Note.—Discussion open until March 1, 1975. To extend the closing date one month, a written request must be filed with the Editor of Technical Publications, ASCE. This paper is part of the copyrighted Journal of the Structural Division, Proceedings of the American Society of Civil Engineers, Vol. 100, No. ST10, October, 1974. Manuscript was submitted for review for possible publication on January 4, 1974.

[1]Prof. of Civ. Engrg., Northwestern Univ., Evanston, Ill.

[2]Struct. Analyst, Alfred Benesch & Co., Chicago, Ill.; formerly, Grad. Student, Dept. of Civ. Engrg., Northwestern Univ., Evanston, Ill.

elements, appears to be more suitable because in narrow and shallow cross sections the transverse distributions can be characterized adequately by fewer parameters than the longitudinal distributions.

Formulation of beam elements for box girders, straight as well as arbitrarily curved in space, seems to have eluded attention so far, and is chosen as the main objective of this study.

Although stability aspects are generally acknowledged to be important in thin-wall box girders, all studies have been confined to local buckling of webs within box girders and no stability analysis of box girders as a whole seems to have been accomplished yet. Therefore, a state of initial stress will be considered herein. Attention will be restricted, however, to the case of small strains and to the linearly elastic behavior. Furthermore, it will be shown that special attention must be devoted to spurious shear effects, a problem thus far known to arise only in bending with shear of beams and shells. A new method of eliminating these effects will be developed herein.

SKEW-ENDED FINITE ELEMENT WITH SHEAR DEFORMATION: ITS GEOMETRY AND KINEMATICS

Computation of the stiffness matrices of curved beam elements is considerably more involved than that of straight elements. Furthermore, with curved beam (or shell) elements it is rather difficult to satisfy exactly the conditions that rigid body rotations cause no self-straining of the element (2,16,22) and that all constant strain states be available. However, curved beams can be approximated by straight finite elements, for which this condition, essential for convergence and good accuracy, is easily satisfied. Nevertheless, in previous studies of highly curved and slender beams, the solutions based on straight elements converged to values that substantially deviated from the correct ones, especially in case of buckling problems (5). This numerical error has been attributed to the neglect of the curvature. For when one assumes the classical bending theory, one implies that the cross sections are normal to the straight element and, thus, the end cross sections of two adjacent elements meeting at an angle are nonparallel and continuity of the beam as a three-dimensional body is not maintained.

However, it is possible to obtain full continuity using straight elements if one adopts the well-known and more accurate theory which allows for transverse shear deformations and does not require the cross sections to be normal to the beam axis, so that the ends of the beam element may be made skew to coincide with the end of the adjacent element meeting at an angle (Fig. 1). One of the objectives herein is to propose such a formulation and to verify that it eliminates the aforementioned numerical error previously encountered at highly curved beams. (This is of interest for finite element solutions of curved beams, plates, and shells in general.)

In the usual approach, when the stiffness matrix of the beam element is determined from the ordinary differential equations of equilibrium or from the expression of potential energy per unit length, it is implied at the outset that the end cross sections are perpendicular to the actual (i.e., curved) beam axis. Therefore, this approach must be abandoned and the element must be treated as three-dimensional.

The geometry of the skew finite element for a box of monosymmetric trapezoidal (skew) cross section (Fig. 1) will now be considered. It is conveniently defined as a mapped image of a parent unit rectangular element of unit square cross

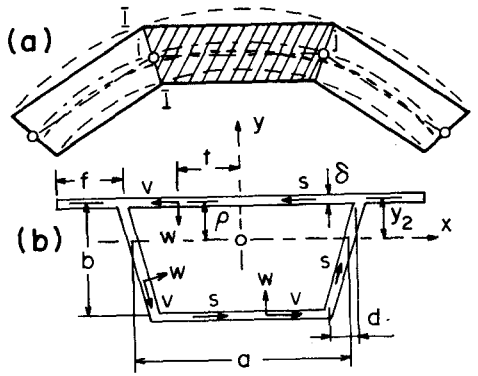

FIG. 1.—(*a*) Subdivision of Curved Beam in Finite Elements; (*b*) Box Cross Section

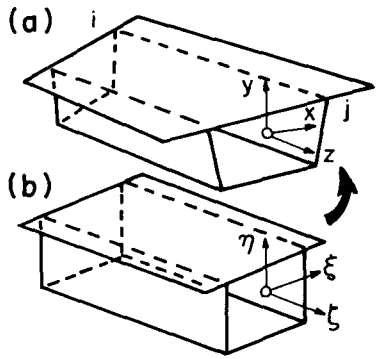

FIG. 2.—(*a*) Finite Element of Box Beam as Mapped Image; (*b*) Parent Unit Box Element

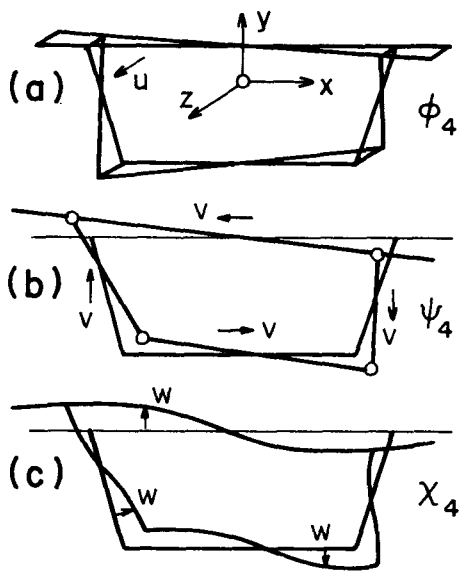

FIG. 3.—(*a*) Longitudinal Warping Mode of Box Cross Section; (*b*) Transverse Distortion Mode, Tangential to Wall; (*c*) Transverse Distortion Mode, Normal to Wall

section and unit length (Fig. 2). Thanks to the straightness, the mapping is linear in each coordinate, i.e.

$$z = \frac{1}{4}(1-\zeta)\,[-l+\xi(1+h\eta)\,a_{z_i}+\eta b_{z_i}]$$

$$+\frac{1}{4}(1+\zeta)\,[l+\xi(1+h\eta)\,a_{z_j}+\eta b_{z_j}] \quad \ldots\ldots\ldots\ldots\ldots\ldots\ldots (1a)$$

$$x = \frac{1}{4}(1-\zeta)\,[\xi(1+h\eta)\,a_{x_i}+\eta b_{x_i}]+\frac{1}{4}(1+\zeta)\,[\xi(1+h\eta)\,a_{x_j}+\eta b_{x_j}] \quad (1b)$$

$$y = \frac{1}{4}(1-\zeta)\,[\xi(1+h\eta)\,a_{y_i}+\eta b_{y_i}]+\frac{1}{4}(1+\zeta)\,[\xi(1+h\eta)\,a_{y_j}+\eta b_{y_j}] \quad (1c)$$

in which x, y, z = local rectangular cartesian coordinates for the skew element (Fig. 2); ξ, η, ζ = coordinates of the parent rectangular element that map into x, y, and z; subscripts i and j refer to the ends of the element and z_i, z_j are their axial coordinates; $h = d/a$, with $2d$ = difference between the top and bottom widths of box (for a rectangular box, $h = 0$); $a_{x_i}, a_{y_i}, \ldots, b_{z_j}$ = components of vectors **a** and **b** that characterize the planes of end cross sections; and magnitudes $a = |\mathbf{a}|$ and $b = |\mathbf{b}|$ represent the width and the depth of box at lines through the centroid (Fig. 1).

The ends of the element, skew with respect to its axis, may (but need not) be made normal to the given curved beam axis. For good accuracy, the element axis is defined so that it deviates to both sides of the given curved beam axis and forms with it equal areas on both sides (Fig. 1).

The mapping in Eqs. 1 is introduced in such a form that $\zeta = \pm 1$ are the end cross sections. In the case of a doubly symmetric box, limits $\xi = \pm 1$ are the sides of the box and limits $\eta = \pm 1$ are its bottom and top. However, in the case of a monosymmetric box (i.e., trapezoidal) it is more convenient to use other limits because the point that is mapped into the centroid does not lie at mid-depth of the parent unit element, i.e., if the coordinates of bottom and top plates, measured from the centroid, are $y_2 - b$ and y_2, one has limits $\eta_2 = 2y_2/b$ and $\eta_1 = \eta_2 - 2$. Furthermore, if the box has overhanging flanges of length f, the limits of ξ at η values for flanges are $\xi_2 = 1 + f/a_2$, $\xi_1 = -\xi_2$, in which $2a_2$ = width of top side of the box.

Furthermore, a linear variation of cross section along the element (tapered beam) can be modeled by appropriate differences of a_{x_i} and b_{y_i} from a_{x_j} and b_{y_j}. Nonparallel top and bottom sides of cross section could also be accommodated, replacing η with $\eta\,(1 + c\,\xi)$ in all b terms of Eq. 1 (c = constant).

All theories of beams are based on assumed basic displacement distributions within the cross section. In conformity with the well-known theories of thin-wall beams of closed cross section (e.g., Refs. 3 and 27) one introduces

$$u = \sum_{k=1}^{4} U_k(z)\,\phi_k(s); \quad v = \sum_{k=1}^{4} V_k(z)\,\psi_k(s); \quad w = \sum_{k=1}^{4} V_k(z)\,\chi_k(s) \quad \ldots\ldots (2)$$

in which z = longitudinal (axial) coordinate; s = coordinate along the walls in the cross section; u = longitudinal displacement of a general point of cross section; v, w = displacements in the cross section plane, tangential and normal to the wall; and

$$\phi_1 = 1; \quad \phi_2 = \frac{a\xi}{2}; \quad \phi_3 = \frac{b\eta}{2}; \quad \phi_4 = \frac{ab\xi\eta}{4}; \quad \psi_1 = \rho(s); \quad \psi_2 = \frac{a\xi_{,s}}{2};$$

$$\psi_3 = \frac{b\eta_{,s}}{2}; \quad \psi_4 = \frac{ab(\xi\eta_{,s} + \eta\xi_{,s})}{4}; \quad \chi_1 = t(s); \quad \chi_2 = \frac{b\eta_{,s}}{2}; \quad \chi_3 = \frac{a\xi_{,s}}{2};$$

$$\chi_4 = \frac{\xi\eta}{4(a\delta_1^3 + b\delta_2^3)}[a^3\delta_1^3(3-\xi^2)\xi_{,s} + b^3\delta_2^3(3-\eta^2)\eta_{,s}] \quad \ldots\ldots\ldots (3)$$

in which subscript s following a comma denotes a derivative with respect to s (in the actual element), e.g., $\xi_{,s} = d\xi/ds$; the expression for χ_4 applies only in the case of a rectangular box; δ_1, δ_2 = thickness of horizontal and vertical sides of box; and ρ = distance of cross-sectional wall tangent from beam axis; t = length of this tangent.

Parameters U_1, V_1, and V_3 represent rigid-body displacements of the whole cross section in the z, x, and y directions; ϕ_1, ψ_2 with χ_2, and ψ_3 with χ_3 = the corresponding displacement distributions; U_2, U_3, and V_1 = rigid-body rotations about axes y, x, and z; ϕ_2, ϕ_3, and ψ_1 with χ_1 = the corresponding distributions.

The remaining U_k and V_k represent deformations of the cross section. Parameter U_4 and distribution ϕ_4 [Fig. 3(*a*)] describe the longitudinal warping mode, such that u varies linearly along each side of the box; V_4 and ψ_4 with χ_4 describe the transverse distortion mode of the box; ψ_4 = the distribution of the tangential displacement, v, due to distortion of the cross section, as proposed by Vlasov [Ref. 27, Fig. 3(*b*)]; χ_4 = the distribution of the normal displacement, w, due to the distortion of the cross section [Fig. 3(*c*)]. It can easily be derived by analyzing the cross section as a continuous frame undergoing unit enforced displacements at its corners. An obvious method to determine χ_4 is the slope-deflection method, which yields χ_4 as given in Eqs. 3. For a rectangular box, the transverse curvature of the wall, caused by distortion in Fig. 3(*b*) with unit bending moments in the corners, is obtained as $k_s = 12\,\xi\,\eta\,\delta^{-3}/(\delta_1^{-2} + \delta_2^{-2})$, in which δ = thickness at the point considered. Integration of this expression yields χ_4 as given in Eqs. 3 because $k_s = d^2w/ds^2 = (d^2\chi_4/ds^2)\,V_4$; and $d^2\chi_k/ds^2 = 0$ for $k < 4$.

Experience has shown that the two deformation modes, U_4, and V_4, are sufficient to characterize the global deformations of a long single-cell box girder. However, for short girders or multiple-cell boxes, and also for local deformation modes of single-cell boxes, a greater number of deformation modes would be required (3).

By increasing the number of terms in Eq. 2, more accurate solutions can be obtained. The corresponding formulations would be an easy extension of the present one. However, it seems that the four terms in Eq. 2 suffice for practical purposes (27) in the case of global behavior of long single-cell box girders.

The internal forces associated with displacement parameters U_k and V_k are

$$P_k = \int_s \phi_k(s)\,p_z\,ds; \quad Q_k = \int_s [\psi_k(s)\,p_s + \chi_k(s)\,p_n]\,ds \quad \ldots\ldots\ldots (4)$$

in which p_z, p_s, and p_n = loads distributed over the area of wall in directions

z, s, and normal n of wall; P_1 = normal force; Q_2 and Q_3 = horizontal and vertical shear force; P_2 and P_3 = bending moments about axes y and z; Q_1 = torque; P_4 = longitudinal bimoment; and Q_4 = transverse bimoment (27).

The assumption of the basic distributions of unknown displacements within the finite element (interpolation or shape functions) is the basis of the finite element approach. Herein one introduces

$$V_k = \frac{1}{2}(1-\zeta)\,V_{k_i} + \frac{1}{2}(1+\zeta)\,V_{k_j}; \quad k = 1, 2, 3, 4 \quad \ldots\ldots\ldots (5a)$$

$$U_k = \frac{1}{2}(\zeta^2-\zeta)\,U_{k_i} + (1-\zeta^2)\,U_{k_0} + \frac{1}{2}(\zeta^2+\zeta)\,U_{k_j}; \quad k = 2, 3, 4 \quad \ldots\ldots (5b)$$

$$U_1 = \frac{1}{2}(1-\zeta)\,U_{1_i} + \frac{1}{2}(1+\zeta)\,U_{1_j}; \quad k = 1 \quad \ldots\ldots\ldots (5c)$$

and the corresponding column matrix of generalized displacements of the element (19×1 in size) is

$$\mathbf{q} = \begin{Bmatrix} \mathbf{q}^b \\ \mathbf{q}^c \end{Bmatrix} \quad \ldots\ldots\ldots (6a)$$

$$\mathbf{q}^b = (V_{1_i}, V_{2_i}, V_{3_i}, V_{4_i}, U_{1_i}, U_{2_i}, U_{3_i}, U_{4_i}, V_{1_j}, V_{2_j}, \ldots U_{4_j})^T \quad \ldots\ldots (6b)$$

$$\mathbf{q}^c = (U_{2_0}, U_{3_0}, U_{4_0})^T \quad \ldots\ldots\ldots (6c)$$

Parameters U_{k_i}, U_{k_j}, V_{k_i}, and V_{k_j} (16 in number) represent generalized cross-sectional displacements U_k and V_k at ends i and j, and the three parameters U_{k_0} grouped in matrix $\mathbf{q}^c$ represent displacements U_k at midlength (i.e., at an interior node) of the element. (Superscript T refers to a transpose.) Consequently, Eqs. 2, 5, and 6 may be lumped in one matrix relation

$$(w, v, u)^T = \mathbf{A}\,\mathbf{q} \quad \ldots\ldots\ldots (7)$$

in which $\mathbf{A} = 3 \times 19$ matrix of interpolation functions (see Eqs. 28).

Elimination of Spurious Shear Stiffness in Bending and Torsion

Note that in Eqs. 5 the transverse displacement parameters and the axial translation are assumed to vary linearly along the element, whereas transverse rotations and warping are taken as quadratic (Fig. 4). This is a departure from the standard approach in bending of beams (21) and in torsion of thin-wall beams (5), in which a cubic variation of transverse displacements is normally being used (Fig. 4) to satisfy the continuity of the transverse rotations expressed as the derivatives of the transverse displacements. By contrast, in the present formulation all rotations are independent of displacements (which is a distinct feature of hybrid finite elements), and so the transverse displacements need not satisfy any such condition and may be considered to be distributed linearly.

Including shear deformations, one faces, in the case of very slender beams, the well-known problem of a large numerical error due to spurious shear stiffness (28), similar to that which occurs in thick-shell elements. With increasing number of elements, i.e., as $l \to 0$, the calculated deformation of the beam under a

TABLE 1.—Critical Bending Moment for Lateral Buckling with Warping of Beam or Arch of Box Cross Section

Number of elements (1)	Straight beam (2)[a]	Arch	
		Maximum (3)[a]	Minimum (4)[a]
16	1.700	2.364	−1.058
32	1.600	2.246	−1.126
80	1.583	2.197	−1.139
exact	1.583	2.197	−1.139

[a]Moments are in inch-pounds × 10^{10}.
Note: 1 in.-lb = 0.1130 N · m.

TABLE 2.—Deflections of Twisted Tapered Box Girder with Distortion and Warping, Compared with Results from Ref. 13

Distance from support, in inches (1)	Test from Ref. 13 (2)[a]	Solution from Ref. 13 (3)[a]	Present method (40 elements) (4)[a]
0	0	0	0
4	0.75	0.68	0.74
8	3.51	3.32	3.48
12	5.56	5.41	5.50
16	7.41	7.39	7.40
20	8.59	8.69	8.59
24	9.07	9.16	9.07

[a]Deflections are in inches × 10^{-3}.
Note: 1 in. = 25.4 mm.

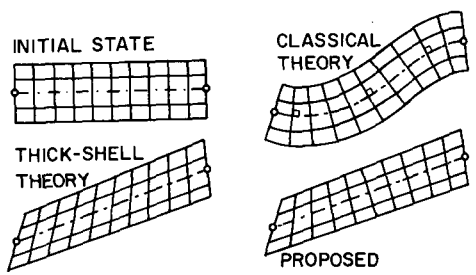

FIG. 4.—Deformation Mode of Proposed Finite Element in Simplest Special Case of Bending with Shear, in Comparison with Other Theories (Classical Theory—Cross Sections Remain Normal)

given load tends to zero, i.e., the beam becomes infinitely stiff. A possible remedy has previously been found in the use of numerical integration formulas of reduced order, i.e., lower than the degree of polynomials in the shape functions (see p. 288, Ref. 28). In the present case, the reduced integration order could probably also be used, but polynomials of higher order would have to be employed in Eqs. 5, with the disadvantage of an increased number of unknown displacement parameters.

Fortunately, numerical experience with the present finite element has indicated that it is free of any spurious shear effects. This appears to be achieved by the fact that the interpolation polynomials for transverse in-plane displacement parameters V_k are of a lower degree (linear) than those for longitudinal displacement parameters U_2, U_3, and U_4 characterizing bending rotations and warping (quadratic). This is manifested by the fact that the element is subparametric [i.e., its geometry is defined by fewer parameters than its deformations (28)] and gives to U_2, U_3, and U_4 extra degrees-of-freedom within the element, as indicated by interior nodes. In the limit case of a very narrow and shallow girder, the extra degrees-of-freedom make it possible for the excess equilibrium conditions associated with the interior nodes to enforce vanishing shear strains and, thus, also the normality of the cross sections (i.e., the condition $U_2 = -dV_2/dz$) in a certain average sense within the element, even though it is violated in general points within the element. Moreover, these conditions also eliminate, in the case of very slender beams, similar spurious shear effects relative to distortion V_4 and warping U_4. Numerical examples further revealed that an isoparametric element, with all distributions linear, could not be used because substantial errors would result in the case of bending or transverse distortion of very slender beams.

The preceding result, which seems to have passed unnoticed so far, has broader implications for beams, plates, and shells, in general, and is considered in more detail by the writers in a subsequent paper. It appears that for elimination of spurious shear effects it is essential that the polynomials for transverse displacement and for bending rotation be of unequal degrees, and that the one for rotation be at least quadratic. If these degrees are 1,2 or 3,2 or 2,3, the spurious shear stiffness does not arise, while for degrees 1,1 or 2,1 or 2,2 or 3,3 it does arise. The degrees of polynomials proposed herein represent the combination which gives the lowest number of displacement parameters of the element. Note also that an isoparametric element would not be free of spurious shear stiffness; one must use a subparametric element.

In contrast to the alternative of numerical integration of reduced order (28), the present formulation not only allows the use of fewer displacement parameters, but also has the advantage of monotonic convergence (upper bound solution), because full continuity between the finite elements is satisfied.

Incremental Stiffness in Presence of Initial Stress

Consider now that the beam is initially in equilibrium at initial normal stresses σ_z^0 and initial shear stresses τ_{zs}^0 in the walls. Subsequently, a small incremental deformation occurs. The virtual work of stresses and loads after incremental deformation upon any kinematically admissible variation of displacements within the finite element is

$$\delta W = \delta W_1 + \delta W_0 - \int_z \int_s (p_z\,\delta u + p_s\,\delta v + p_n\,\delta w)\,ds\,dz \quad \ldots\ldots\ldots\ldots (8)$$

in which

$$\delta W_1 = \int_z \int_A \sigma_z\,\delta e_z\,dA\,dz + \int_z \int_A \tau_{zs}\,\delta e_{zs}\,dA\,dz + \int_z \int_s m_s\,\delta k_s\,ds\,dz \quad \ldots\ldots (9)$$

$$\delta W_0 = \int_z \int_A \sigma^0_z\,\delta \epsilon_z\,dA\,dz + \int_z \int_A \tau^0_{zs}\,\delta \gamma_{zs}\,dA\,dz \quad \ldots\ldots\ldots\ldots\ldots (10)$$

in which δW_1 = virtual work due to incremental stresses; δW_0 = virtual work due to initial stresses; A = area of cross section; m_s and k_s = transverse bending moment and transverse curvature of wall; $k_s = d^2w/ds^2$; e_z, e_{zs} = small (linearized) normal strain and shear strain; ϵ_z and γ_{zs} = finite normal and shear strains, i.e.

$$\left.\begin{aligned} e_z &= \frac{\partial u}{\partial z}; \quad \epsilon_z = e_z + \frac{1}{2}\left(\frac{\partial v}{\partial z}\right)^2 + \frac{1}{2}\left(\frac{\partial w}{\partial z}\right)^2 \\ e_{zs} &= \frac{\partial u}{\partial s} + \frac{\partial v}{\partial z}; \quad \gamma_{zs} = e_{zs} + \frac{1}{2}\frac{\partial v}{\partial s}\frac{\partial v}{\partial z} + \frac{1}{2}\frac{\partial w}{\partial s}\frac{\partial w}{\partial z} \end{aligned}\right\} \quad \ldots\ldots\ldots (11)$$

Eq. 9 contains small strain because only infinitesimally small incremental deformation is considered. Nevertheless, in product $\sigma^0_z\,\delta\epsilon_z$ (Eq. 10) the finite strain expression must be used because, in view of σ^0_z and τ^0_{zs} being finite (large), product $\sigma^0_z\,\delta e_z$ would be accurate only up to small quantities of first order in displacement gradients, whereas product $\sigma_z\,\delta e_z$ (Eq. 9) is a small quantity of second order (e.g., Ref. 4). Component $(\partial u/\partial z)^2$ has been deleted from ϵ_z since for small incremental strains it is negligible with regard to e_z. Similar comments can be made about $\tau_{zs}\delta e_{zs}$ and $\tau^0_{zs}\delta\gamma_{zs}$. (The work of initial transverse bending moments in the wall includes no second-order small term.)

$$\mathbf{e} = (e_z, e_{zs}, k_s)^T; \quad \underset{\sim}{\sigma} = (\sigma_z, \tau_{zs}, m_s)^T \quad \ldots\ldots\ldots\ldots\ldots (12)$$

$$\mathbf{u}' = \left(\frac{\partial u}{\partial z}, \frac{\partial u}{\partial x}, \frac{\partial u}{\partial y}, \frac{\partial v}{\partial z}, k_s\right)^T; \quad \hat{\mathbf{u}} = \left(\frac{\partial u}{\partial \zeta}, \frac{\partial u}{\partial \xi}, \frac{\partial u}{\partial \eta}, \frac{\partial v}{\partial \zeta}, \frac{\partial v}{\partial \xi}, \frac{\partial v}{\partial \eta}, k_s\right) \quad (13)$$

and to define matrices $\mathbf{h}$, $\mathbf{d}$, $\mathbf{g}$, $\mathbf{c}_1$, and $\mathbf{c}_2$ by the relations

$$\mathbf{e} = \mathbf{h}\,\mathbf{u}'; \quad \mathbf{u}' = \mathbf{d}\,\hat{\mathbf{u}}; \quad \hat{\mathbf{u}} = \mathbf{g}\,\mathbf{q}; \quad \partial v/\partial z = \mathbf{c}_1\mathbf{q}; \quad \partial w/\partial z = \mathbf{c}_2\mathbf{q} \quad \ldots\ldots (14)$$

Matrix $\mathbf{d}$ is derived from the relation

$$\begin{Bmatrix} \frac{\partial u}{\partial \zeta} \\ \frac{\partial u}{\partial \xi} \\ \frac{\partial u}{\partial \eta} \end{Bmatrix} = \begin{bmatrix} \frac{\partial z}{\partial \zeta}, & \frac{\partial x}{\partial \zeta}, & \frac{\partial y}{\partial \zeta} \\ \frac{\partial z}{\partial \xi}, & \frac{\partial x}{\partial \xi}, & \frac{\partial y}{\partial \xi} \\ \frac{\partial z}{\partial \eta}, & \frac{\partial x}{\partial \eta}, & \frac{\partial y}{\partial \eta} \end{bmatrix} \begin{Bmatrix} \frac{\partial u}{\partial z} \\ \frac{\partial u}{\partial x} \\ \frac{\partial u}{\partial y} \end{Bmatrix} = \mathbf{J} \begin{Bmatrix} \frac{\partial u}{\partial z} \\ \frac{\partial u}{\partial x} \\ \frac{\partial u}{\partial y} \end{Bmatrix} \quad \ldots\ldots\ldots (15)$$

in which $\mathbf{J}$ = Jacobian matrix of the mapping defined by Eq. 1, and from a similar relation that holds for the derivatives of v. Matrix $\mathbf{d}$ (5×7 in size) obviously consists of the components, J^{-1}_{ij}, of the inverse matrix, $\mathbf{J}^{-1}$:

$$\mathbf{d} = \left[\begin{array}{c|cccc} \mathbf{J}^{-1} & \underset{\sim}{0} & \underset{\sim}{0} & \underset{\sim}{0} & \underset{\sim}{0} \\ \hline \underset{\sim}{0} & J^{-1}_{11} & J^{-1}_{12} & J^{-1}_{13} & 0 \\ \underset{\sim}{0} & 0 & 0 & 0 & 1 \end{array}\right] \quad \ldots\ldots\ldots (16)$$

Matrices $\mathbf{g}$, $\mathbf{c}_1$ and $\mathbf{c}_2$ follow from Eq. 7 (for details see Appendix I). The stress-strain law and the strain-displacement relations may be written as

$$\underset{\sim}{\sigma} = \mathbf{D}\,\mathbf{e}; \quad \mathbf{e} = \mathbf{B}\,\mathbf{q}, \quad \text{with} \quad \mathbf{B} = \mathbf{h}\,\mathbf{d}\,\mathbf{g} \quad \ldots\ldots\ldots\ldots\ldots (17)$$

Here $\mathbf{D}$ = 3×3 elastic matrix in which $D_{ij} = 0$ for $i \neq j$; $D_{11} = E$ = Young's modulus; $D_{22} = G$ = shear modulus; and $D_{33} = D_s$ = cylindrical bending stiffness of walls ($D_s = m_s/k_s = E\delta^3/12\,(1-\nu)$; ν = Poisson ratio).

Using Eqs. 16 and 13, Eq. 9 can be brought to the form

$$\delta W_1 = \int_z \int_A \delta \mathbf{e}^T \underset{\sim}{\sigma}\,dz\,dA = \delta \mathbf{q}^T \mathbf{K}^1 \mathbf{q} \quad \ldots\ldots\ldots\ldots\ldots (18)$$

$$\text{with} \quad \mathbf{K}^1 = \int_z \int_A \mathbf{B}^T \mathbf{D}\,\mathbf{B}\,dz\,dA = \int_{-1}^{1} \int_{\eta_1}^{\eta_2} \int_{\xi_1}^{\xi_2} \mathbf{B}^T \mathbf{D}\,\mathbf{B}\,|J|\,d\xi\,d\eta\,d\zeta \quad \ldots\ldots (19)$$

in which $|J|$ = det ($\mathbf{J}$) = Jacobian. From the form of Eq. 18 it is apparent that $\mathbf{K}^1$ is the stress-independent part of the incremental (tangential) stiffness matrix (of size 19×19) of the finite element. In the general case, the integrals in Eq. 19 must be evaluated numerically, for which Gaussian-point integration (of order 8, with nine points; Ref. 28) is adequate. In special cases, explicit integration is possible (see Eq. 31).

Initial stresses will be assumed, for the sake of simplicity, to be caused only by initial axial force P^0 (positive for tension) and by initial bending moment M^0_x about centroidal axis. Thus

$$\sigma^0_z = \frac{P^0}{A} + \frac{M^0_x}{I_x}\,y \quad \ldots\ldots\ldots\ldots\ldots\ldots\ldots\ldots (20)$$

and τ^0_{zs} will be considered zero. Using $\mathbf{c}_1$ and $\mathbf{c}_2$ from Eq. 14, Eq. 10 (with $\tau^0_{zs} = 0$) takes the form:

$$\delta W_0 = \int_z \int_A \sigma^0_z\,[(\mathbf{c}_1\,\delta\mathbf{q})^T \mathbf{c}_1\mathbf{q} + (\mathbf{c}_2\,\delta\mathbf{q})^T \mathbf{c}_2\mathbf{q}]\,dz\,dA + \delta_0 \quad \ldots\ldots\ldots (21a)$$

$$\text{or} \quad \delta W_0 = \int_z \int_A \sigma^0_z\,\delta\mathbf{q}^T \mathbf{c}^T\mathbf{c}\mathbf{q}\,dz\,dA + \delta_0 = \delta\mathbf{q}_T \mathbf{K}^0\mathbf{q} + \delta_0 \quad \ldots\ldots\ldots (21b)$$

in which $\mathbf{c} = [\mathbf{c}_1, \mathbf{c}_2]$ and

$$\mathbf{K}^0 = \frac{P^0}{A}\int_{-1}^{1}\int_{\eta_1}^{\eta_2}\int_{\xi_1}^{\xi_2}\mathbf{c}^T\mathbf{c}|J|d\xi d\eta d\zeta + \frac{M_x^0}{I_x}\int_{-1}^{1}\int_{\eta_1}^{\eta_2}\int_{\xi_1}^{\xi_2}\mathbf{c}^T\mathbf{c}|J|d\xi d\eta d\zeta \quad . \quad . \quad . \quad (22)$$

and δ_0 is an expression which does not contain $\mathbf{q}$ and is thus irrelevant for stiffness. From the form of Eq. 21 it is clear that $\mathbf{K}^0$ is the stress-dependent part of the incremental stiffness matrix of the element.

The virtual work may now be expressed as $\delta W = \delta\mathbf{q}^T(\mathbf{K}^1\mathbf{q} + \mathbf{K}^0\mathbf{q} - \mathbf{F})$, in which $\mathbf{F} = 19 \times 1$ column matrix of applied forces, associated with $\mathbf{q}$. The condition that δW vanish for any $\delta\mathbf{q}$ yields the incremental equilibrium condition of the element

$$\mathbf{K}\mathbf{q} = \mathbf{F}, \quad \text{with} \quad \mathbf{D} = \mathbf{K}^1 + \mathbf{K}^0 \quad . \quad (23)$$

To isolate the components associated with internal node c of the element (referred to by subscript 0), element stiffness matrix $\mathbf{K}$ and load matrix $\mathbf{F}$ may be partitioned similarly to the way $\mathbf{q}$ is partitioned in Eq. 6. Eq. 23 then becomes

$$\left[\begin{array}{c|c} \mathbf{K}_{bb} & \mathbf{K}_{bc} \\ \hline \mathbf{K}_{cb} & \mathbf{K}_{cc} \end{array}\right]\left\{\begin{array}{c} \mathbf{q}^b \\ \hline \mathbf{q}^c \end{array}\right\} = \left\{\begin{array}{c} \mathbf{F}_b \\ \hline \mathbf{F}_c \end{array}\right\} \quad . \quad (24)$$

Elimination of all three components of $\mathbf{q}_c$, which is known as the static condensation procedure (21), yields

$$\mathbf{q}^c = -\mathbf{K}_{cc}^{-1}\mathbf{K}_{cb}\mathbf{q}^b + \mathbf{K}_{cc}^{-1}\mathbf{F}_c; \quad \text{and} \quad \mathbf{k}\mathbf{q}^b = \mathbf{f} \quad . \quad . \quad . \quad . \quad . \quad . \quad . \quad . \quad . \quad . \quad . \quad . \quad . \quad . \quad . \quad . \quad . \quad (25)$$

$$\text{in which} \quad \mathbf{k} = \mathbf{K}_{bb} - \mathbf{K}_{bc}\mathbf{K}_{cc}^{-1}\mathbf{K}_{cb}; \quad \mathbf{f} = \mathbf{F}_b - \mathbf{K}_{bc}\mathbf{K}_{cc}^{-1}\mathbf{F}_c \quad . \quad . \quad . \quad . \quad . \quad . \quad . \quad . \quad . \quad . \quad (26)$$

Matrix $\mathbf{k}$ is a 16×16 incremental stiffness matrix of the element, referred solely to its boundary nodes, and $\mathbf{f}$ = the associated 16×1 column matrix of applied forces. Inverse $\mathbf{K}_{cc}^{-1}$ is very simple (because $\mathbf{K}_{cc}$ is a diagonal matrix, in the case of uniform cross sections) and explicit expressions are possible.

To obtain the stiffness matrix of the whole structure, one must superimpose all element stiffness matrices transformed to global coordinates. These matrices have the form $\mathbf{T}^T\mathbf{k}\,\mathbf{T}$, in which $\mathbf{T}$ = transformation matrix from element coordinates x, y, and z to global coordinates X, Y, and Z.

Obviously, in assembling the structural stiffness matrix one can easily include stiffness matrices of transverse diaphragms, which are the same as those for plate elements.

Numerical Examples

The accuracy of the proposed method of analysis is examined by solving some practical problems (on CDC-6400 in single precision arithmetic). The solutions are carried out for various numbers n of finite elements and are compared with the exact analytical solutions of the differential equation, when possible.

Lateral Buckling of Beam with Rigid Cross Section.—The critical moment, M_x^0, for a simply-supported beam, restrained against twist but free to warp at ends, is calculated. The beam is of depth b = 120 in. (3,050 mm), width a = 50 in. (1,270 mm), has flanges of thickness δ_2 = 2.4 in. (61.0 mm), and webs of thickness δ_1 = 2.0 in. (50.8 mm). Modulus of elasticity $E = 30 \times 10^6$ psi (207,000 MN/m^2) and shear modulus $G = E/3$. The numerical values are compared with the exact analytical solution of the Euler differential equation (Appendix II) associated with the preceding expression for δW (see Table 1).

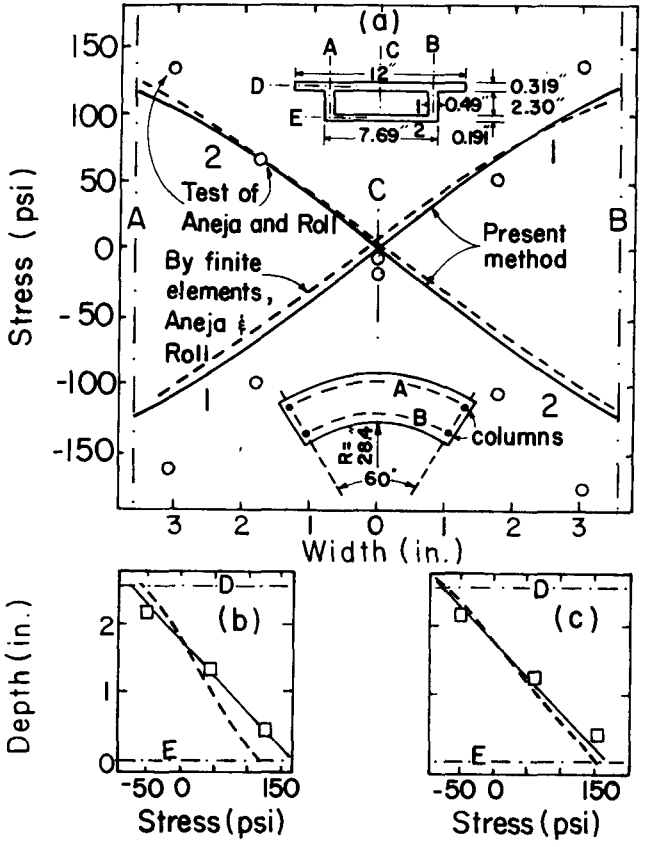

FIG. 5.—Comparison of Stresses from Present Solution with Test Data of Ref. 1 and their Finite Element Solution: (*a*) Radial Stresses at Interior (Line 1) and Exterior (Line 2) Surfaces of Bottom Flange; (*b*) Longitudinal Stresses at Midthickness of Inner Vertical Web; (*c*) Longitudinal Stresses at Midthickness of Outer Vertical Web (1 psi = 6.9 N/m^2; 1 in. = 25.4 mm)

Lateral Buckling of Circular Arch with Rigid Cross Section.—The critical moment, M_x^0, for a pin-ended arch, restrained against twist but free at ends, is calculated. The arch is of depth b = 120 in. (3,050 mm), a = 50 in. (1,270 mm), radius R = 1,833 in. (46.56 m), and central angle 60°. The flanges of

thickness δ_2 = 2.4 in. (61.0 mm), and the webs have thickness δ_1 = 2.0 in. (50.8 mm). Modulus of elasticity $E = 30 \times 10^6$ psi (207,000 MN/m^2) and shear modulus $G = E/3$. Comparison with the exact analytical solution of the differential equation (Appendix I) is given in Table 1.

Bimoment Decay along Box Beam.—The wall is assumed to be very thin, i.e., $V_1 \approx 0$. A simply-supported beam restrained against distortion is loaded at its ends by longitudinal forces (without static resultant) giving a bimoment of 100 N · m^2; span = 1 m, depth b = 120 cm, width a = 70 cm, and δ_2 = 1.6 cm, δ_1 = 1 cm. The value of the bimoment at midspan, calculated according to p. 248 of Ref. 27, is 81 N · m^2; 32 elements yield the same result.

Axisymmetric Buckling of Cylindrical Shell.—Using the same example given on p. 459 of Ref. 24, critical stress $\sigma_z = \sigma_{cr}$ causing axisymmetric buckling of a cylindrical shell of diameter a and thickness h (with ratio a/h = 303) is 60,000 psi (414 N/mm^2). Using the analogy with a beam on elastic foundation (and the matrix in Eq. 31), the same result is obtained with 40 elements.

Distortion of Tapered Bridge Box Girder.—The case previously studied by Křístek (13), both numerically and experimentally with a PVC model, is analyzed. The model is a simply-supported tapered box girder of span 48 in. (1,220 mm), width 4 in. (102 mm), and of a depth varying parabolically from 4.7 in. (119 mm) at the supports to 3.2 in. (81.3 mm) at the midspan. At the ends, distortion and warping are prevented. The wall thickness is 0.02 in. (0.508 mm), $E = 0.5 \times 10^6$ psi (3,450 MN/m^2), and $G = E/2.66$. The girder is loaded by a pair of distributed loads along the diagonal of the box. The loads have a uniform vertical component, q_z = 0.716 lb/in. (175 N/m). Normal displacements w at various points along the span are evaluated (see Table 2).

Horizontally Curved Box Girder in Bending and Torsion with Distortion and Warping.—The case previously studied by Aneja and Roll (1), with a Plexiglas 11-UVA model and with the finite element method, is considered herein (see Fig. 5). (All values in Fig. 5 are for midspan. Squares are data points for midthickness, obtained as averages of the surface readings from Ref. 1.) The model is loaded by a centric live load of 0.494 psi (3,410 N/m^2). The stress distributions within the midspan cross section, as obtained with the present method, are compared with the results from Ref. 1 in Table 2.

It has also been checked that the present finite element gives the correct solutions for plane bending and buckling of straight beams, rings and arches, both thick and slender.

Conclusions

1. A method for the analysis of the global behavior of long curved or straight box girders under initial stress is presented. It is based on thin-wall beam elements, including the modes of warping and distortion of cross section. The cross section must consist of a single cell, may have overhangs, and may be variable along the girder. The method is an extension and refinement of the method presented in Ref. 5.

2. The spurious shear effects due to transverse bimoment, along with those due to shear forces, are eliminated by virtue of the fact that the interpolation polynomials for transverse displacements and distortions are of lower order

than those for bending rotations and torsional warping, thus providing for interior nodes excess equilibrium conditions which can enforce vanishing shear strains in the limiting case of very slender girders. The element is subparametric. The spurious shear effects also could probably be removed by numerical integration of reduced order (29), but an element with a greater number of degrees-of-freedom would then be required.

3. The beam element of any shape is regarded as a mapped image of one parent unit element. Explicit expressions for the stiffness matrix are possible only in the case of a straight girder of rectangular cross section. Generally, the stiffness matrix is evaluated by a Gaussian numerical integration formula.

4. Numerical examples demonstrated good agreement with analytical solutions as well as experimental data.

5. The finite element gives monotonic convergence (upper-bound solutions) to the exact solutions of the differential equation of the problem.

6. The present type of interpolation polynomials and the skewness of the ends of the element, the typical features of the present formulation, can also be applied to thin-wall beams of open cross section to eliminate the numerical error that has previously occurred in finite element solutions of slender, highly curved beams (5).

Acknowledgment

The computing funds, provided by Northwestern University, Evanston, Ill., are gratefully acknowledged.

Appendix I.—Detailed Forms of Matrices

For a beam having a rectangular cross section and a planar curvature in the z-y plane, the following explicit expressions are possible.

Matrix **J** (Jacobian): $4J_{11} = 2l + \eta(b_{z_i} - b_{z_j})$; $4J_{13} = \eta(b_{y_i} - b_{y_j})$; $J_{22} = (1/2)a$; $4J_{31} = (1 - \zeta)b_{z_i} + (1 + \zeta)b_{z_j}$; $4J_{33} = (1 - \zeta)b_{y_i} + (1 + \zeta)b_{y_j}$; all other terms = 0; and l = length of element. The determinant is $|J| = J^* \, a/2$ and $J^* = (1/8)\,[l\,(b_{y_j} + b_{y_i}) + \zeta l(b_{y_j} - b_{y_i}) + \eta(b_{y_i} b_{z_j} - b_{y_j} b_{z_i})]$. In particular, for a straight beam, $J_{11} = (1/2)\,l$; $J_{22} = (1/2)\,a$; $J_{33} = (1/2)\,b$; and $J^* = (1/4)\,bl$. The inverse is $\mathbf{J}^{-1} = \hat{\mathbf{J}}/J^*$, in which $\hat{J}_{11} = J_{33}$; $\hat{J}_{13} = -J_{13}$; $J_{22} = J^*/J_{22}$; $\hat{J}_{31} = -J_{31}$; $\hat{J}_{33} = J_{11}$; and all other terms = 0.

Matrix **A** (of interpolation functions, Eq. 7; size 3 × 19):

$$\mathbf{A} = \begin{bmatrix} \mathbf{A}_{01} & \underset{\sim}{0} & \mathbf{A}_{02} & \underset{\sim}{0} & \underset{\sim}{0} \\ \mathbf{A}_1 & \underset{\sim}{0} & \mathbf{A}_2 & \underset{\sim}{0} & \underset{\sim}{0} \\ \underset{\sim}{0} & \mathbf{A}_3 & \underset{\sim}{0} & \mathbf{A}_4 & \mathbf{A}_5 \end{bmatrix} \quad \ldots\ldots\ldots\ldots (27)$$

in which

$$4\mathbf{A}_{01} = [2t(1-\zeta),\ -b\eta_{,s}(1-\zeta),\ a\xi_{,s}(1-\zeta),\ 2\chi_4(1-\zeta)];$$

$$4\mathbf{A}_{02} = [2t(1-\zeta),\ -b\eta_{,s}(1+\zeta),\ a\xi_{,s}(1+\zeta),\ 2\chi_4(1+\zeta)];$$

$$4\mathbf{A}_1 = \left[2\rho(1-\zeta), a\xi_{,s}(1-\zeta), b\eta_{,s}(1-\zeta), \frac{1}{2}ab\,s'(1-\zeta)\right];$$

$$4\mathbf{A}_2 = \left[2\rho(1+\zeta), a\xi_{,s}(1+\zeta), b\eta_{,s}(1+\zeta), \frac{1}{2}ab\,s'(1+\zeta)\right];$$

$$4\mathbf{A}_3 = \left[2(1-\zeta), -a\xi\zeta(1-\zeta), -b\eta\zeta(1-\zeta), -\frac{1}{2}ab\xi\eta\zeta(1-\zeta)\right];$$

$$4\mathbf{A}_4 = \left[2(1+\zeta), a\xi\zeta(1+\zeta), b\eta\zeta(1+\zeta), \frac{1}{2}ab\xi\eta\zeta(1+\zeta)\right];$$

$$4\mathbf{A}_5 = [2a\xi(1-\zeta^2), 2b\eta(1-\zeta^2), ab\xi\eta(1-\zeta^2)] \quad \ldots\ldots\ldots\ldots \quad (28)$$

in which $\rho = (1/2)\,a\xi \sin\alpha - (1/2)\,b\eta\cos\alpha$; $t = (1/2)\,a\xi\cos\alpha + (1/2)\,b\eta\sin\alpha$; $s' = \eta\xi_{,s} + \xi\eta_{,s}$; $\xi_{,s} = (2/a)\cos\alpha$; $\eta_{,s} = (2/b)\sin\alpha$; and $\alpha = 0$ along ξ and $\alpha = 90°$ along η.

Matrix **B** (size 3×19, Eq. 17); Denote $\mathbf{B} = \mathbf{P}/J^*$. Then

$$P_{1\,5} = -\frac{1}{2}J_{33};\quad P_{1\,6} = -\frac{1}{4}a\xi J_{33}(1-2\zeta);\quad P_{1\,7} = -\frac{1}{4}b\eta J_{33}(1-2\zeta)$$

$$+\frac{1}{4}bJ_{13}\zeta(1-\zeta);\quad P_{1\,8} = -\frac{1}{8}ab\xi\eta J_{33}(1-2\zeta) + \frac{1}{8}ab\xi J_{13}\zeta(1-\zeta);$$

$$P_{1\,13} = \frac{1}{2}J_{33};\quad P_{1\,14} = \frac{1}{4}a\xi J_{33}(1+2\zeta);\quad P_{1\,15} = \frac{1}{4}b\eta J_{33}(1+2\zeta)$$

$$-\frac{1}{4}bJ_{13}\zeta(1+\zeta);\quad P_{1\,16} = \frac{1}{8}ab\xi\eta J_{33}(1+2\zeta) - \frac{1}{8}ab\xi J_{13}\zeta(1+\zeta);$$

$$P_{1\,17} = -a\xi J_{33}\zeta;\quad P_{1\,18} = -b\eta J_{33}\zeta - \frac{1}{2}bJ_{13}(1-\zeta^2);\quad P_{1\,19} = -ab\xi\eta J_{33}\zeta$$

$$-\frac{1}{2}ab\xi J_{13}(1-\zeta^2);\quad P_{2\,1} = -\frac{1}{2}\rho J_{33} + \frac{1}{4}b\cos\alpha J_{13}(1-\zeta);$$

$$P_{2\,2} = -\frac{1}{4}a\xi_{,s}J_{33};\quad P_{2\,3} = -\frac{1}{4}b\eta_{,s}J_{33};\quad P_{2\,4} = -\frac{1}{8}abs'J_{33};$$

$$P_{2\,5} = \frac{1}{2}\eta_{,s}J_{33}J_{31};\quad P_{2\,6} = \frac{1}{4}a\xi\eta_{,s}J_{33}J_{31}(1-2\zeta) - \frac{1}{4}a\xi_{,s}J^*\zeta(1-\zeta);$$

$$P_{2\,7} = \frac{1}{4}b\eta\eta_{,s}J_{33}J_{31}(1-2\zeta) - \frac{1}{4}b\eta_{,s}J_{33}J_{11}\zeta(1-\zeta);\quad P_{2\,8} =$$

$$\frac{1}{8}ab\xi\eta\eta_{,s}J_{33}J_{31}(1-2\zeta) - \frac{1}{8}ab\eta\xi_{,s}J^*\zeta(1-\zeta) - \frac{1}{8}ab\xi\eta_{,s}J_{33}J_{11}\zeta(1-\zeta);$$

$$P_{2\,9} = \frac{1}{2}\rho J_{33} + \frac{1}{4}b\cos\alpha J_{31}(1+\zeta);\quad P_{2\,10} = \frac{1}{4}a\xi_{,s}J_{33};$$

$$P_{2\,11} = \frac{1}{4}b\eta_{,s}J_{33};\quad P_{2\,12} = \frac{1}{8}abs'J_{33};\quad P_{2\,13} = -\frac{1}{2}\eta_{,s}J_{33}J_{31};$$

$$P_{2\,14} = -\frac{1}{4}a\xi\eta_{,s}J_{33}J_{31}(1+2\zeta) + \frac{1}{4}a\xi_{,s}J^*\zeta(1+\zeta);$$

$$P_{2\,15} = -\frac{1}{4}b\eta\eta_{,s}J_{33}J_{31}(1+2\zeta) + \frac{1}{4}b\eta_{,s}J_{33}J_{11}\zeta(1+\zeta);\quad P_{2\,16} =$$

$$-\frac{1}{8}ab\xi\eta_{,s}J_{33}J_{31}(1+2\zeta) + \frac{1}{8}ab\eta\xi_{,s}J^*\zeta(1+\zeta) + \frac{1}{8}ab\xi\eta_{,s}J_{33}J_{11}\zeta(1+\zeta);$$

$$P_{2\,17} = a\xi\eta_{,s}J_{33}J_{31}\zeta + \frac{1}{2}a\xi_{,s}J^*(1-\zeta^2);\quad P_{2\,18} = b\eta\eta_{,s}J_{33}J_{31}\zeta$$

$$+\frac{1}{2}b\eta_{,s}J_{11}J_{33}(1-\zeta^2);\quad P_{2\,19} = \frac{1}{2}ab\xi\eta\eta_{,s}J_{33}J_{31} + \frac{1}{4}ab\eta\xi_{,s}J^*(1-\zeta^2)$$

$$+\frac{1}{4}ab\xi\eta_{,s}J_{33}J_{11}(1-\zeta^2);\quad P_{3\,4} = \frac{1}{2}K_s(1-\zeta)J^*;\quad P_{3\,12} = \frac{1}{2}K_s(1+\zeta)J^*;$$

$$K_s = \frac{12\xi\eta}{\delta^3}(b\delta_1^3 + a\delta_2^3) \quad \ldots\ldots\ldots\ldots\ldots\ldots\ldots\ldots \quad (29)$$

and all other terms = 0.

Matrix **c** (size 19×2, Eq. 21): Denote $\mathbf{c} = \{\mathbf{c}_1, \mathbf{c}_2\} = \mathbf{C}/J^*$. Then

$$C_{1\,1} = -\frac{\rho}{2}J_{33} + \frac{3}{2}\cos\alpha;\quad C_{2\,1} = -\frac{t}{2}J_{33} - \frac{\chi_{4,\eta}}{2}J_{13}(1-\zeta);\quad C_{1\,2} = -C_{1\,10}$$

$$= -C_{2\,3} = C_{2\,11} = -\frac{a}{4}\xi_{,s}J_{33};\quad C_{1\,3} = -C_{1\,11} = -C_{2\,2} = C_{2\,10} = -\frac{b}{4}\eta_{,s}J_{33};$$

$$C_{1\,4} = -C_{1\,12} = -\frac{abs}{8}J_{33};\quad C_{2\,4} = -C_{2\,12} = -\frac{\chi_4}{2}J_{33};\quad C_{1\,9} = \frac{\rho}{2}J_{33}$$

$$+\frac{3}{2}\cos\alpha;\quad C_{2\,9} = \frac{t}{2}J_3 + \frac{\chi_{4,\eta}}{2}J_{13}(1+\zeta) \quad \ldots\ldots\ldots\ldots\ldots \quad (30)$$

and all other terms are zero.

Stiffness Matrix for Distortion and Warping of Straight Beams.—Employing static condensation, the stiffness matrix associated with displacement vector $(V_{4_i}, U_{4_i}, V_{4_j}, U_{4_j})$ and force vector (Q_i, B_i, Q_j, B_j) is obtained as:

$$\begin{bmatrix} \frac{60a_0 + b_1 l^2}{6l^3(1+\Phi)} + \frac{cl}{3} & -\frac{60a_0 + b_1 l^2}{12l^2(1+\Phi)} & \frac{\left(\frac{13}{3}+\Phi\right)a_0 + \frac{b_1 l^2}{8}}{l(1+\Phi)} \\ \text{Symm.} & & \end{bmatrix}$$

$$\begin{bmatrix} -\frac{60a_0 + b_1 l^2}{6l^3(1+\Phi)} & \frac{60a_0 + b_1 l^2}{12l^2(1+\Phi)} & \frac{\left(\frac{2}{3}-\Phi\right)a_0 - \frac{b_1 l^2}{24}}{l(1+\Phi)} \\ \frac{60a_0 + b_1 l^2}{12l^2(1+\Phi)} & \frac{60a_0 + b_1 l^2}{12l^2(1+\Phi)} & \frac{\left(\frac{13}{3}+\Phi\right)a_0 + \frac{b_1 l^2}{8}}{l(1+\Phi)} \\ \frac{60a_0 + b_1 l^2}{6l^3(1+\Phi)} + \frac{cl}{3} & & \end{bmatrix} \quad \ldots\ldots\ldots\ldots (31)$$

in which $\Phi = 10\, a_0/b_1 l^2$; $a_0 = EA\, a^2 b^2/48$; and $b_1 = Gab\,(a\delta_1 + b\delta_2)/2$; $c = 8E/\delta\,(1-\nu^2)\,(b/\delta_1^3 + a/\delta_2^3)$. Note that in the nominators of all elements in this matrix the terms containing b_1 become negligible for $l \to 0$, as compared with the terms containing a_0. This is not so in the formulations exhibiting spurious shear stiffness. The matrix in Eq. 31 is of a form exactly analogous to that which relates to displacements $(V_{3_i}, U_{3_i}, V_{3_j}, U_{3_j})$, i.e., to bending deflections and rotations.

Appendix II.—Some Analytical Solutions

Consider now lateral buckling of a straight simply-supported box girder which exhibits longitudinal warping but no distortion of cross sections ($V_4 = 0$) and no shear deformations in bending ($GA_w \to \infty$). The Euler differential equations associated with Eqs. 8 and 10 for δW are obtained, bu a routine procedure, in the form

$$EI_y V_2''' + M_x^0 V_1'' = 0; \quad a_0 U_4'' - b_1 U_4 - b_2 V_1' = 0;$$
$$_2 V_4' + b_1 V_1'' - M_x^0 V_2'' = 0 \quad \ldots\ldots\ldots\ldots\ldots\ldots\ldots\ldots (32)$$

in which $a_0 = \int_A \phi_4^2\, dA$; $b_1 = \int_A (d\phi_4/ds)^2\, dA$; $b_2 = \int_A (d\phi_4/ds)(d\phi_1/ds) dA$; and $(\,)' = d/dz$. Introducing function $f(z)$ such that $f' = U_4$, one obtains $V_1 = (a_0 f'' - b_1 f)/b_2$ and Eqs. 32 can be reduced to the form $f'''' - 2\alpha f'' - \beta f = 0$, with $2\alpha = k^2/l^2 - M_x^{0^2}/b_1 EI_y$ and $\beta = M_x^{0^2}/aEI_y$. Assuming M_x^0 constant along the beam, the solution of this differential equation for boundary conditions $V_1 = U_4' = f = f'' = 0$ at $z = 0$ and $z = L$ is $(\alpha^2 + \beta)^{1/2} - \alpha = \pi^2/L^2$, which yields

$$M_x^0 = \frac{\pi}{L}\left[EI_y GI_s\left(1 + \frac{\pi^2 a}{L^2 GI_s}\right)\left(1 + \frac{\pi^2 a}{L^2 b_1}\right)\right. \quad \ldots\ldots\ldots (33)$$

This expression, apparently not available in the literature, [illegible]ar to that for lateral buckling of beams of open cross section (26).

Utilizing this similarity, which also holds for the corresponding differential equations, the critical bending moment, M_x^0, for a circular arch (of radius R) can be most simply obtained directly from Vlasov's expression for an arch of open cross section (27). Thus

$$M_x^0 = \alpha \pm \sqrt{\alpha^2 + \beta} \quad \ldots\ldots\ldots\ldots\ldots\ldots\ldots\ldots (34)$$

$$\text{in which} \quad 2R\alpha = EI_y + \left(GI_s + \frac{\pi^2}{L^2} a\right)\left(1 + \frac{\pi^2 a}{L^2 b_1}\right)^{-1} \quad \ldots\ldots\ldots (35a)$$

$$\beta = EI_y GI_s \left(\frac{\pi^2}{L^2} - \frac{1}{R^2}\right)\left(1 + \frac{\pi^2 a}{L^2 GI_s}\right)\left(1 + \frac{\pi^2 a}{L^2 b_1}\right)^{-1} \quad \ldots\ldots\ldots (35b)$$

For the general differential equations of equilibrium in terms of U_k and V_k, in absence of initial stress, see Eq. 9 of Ref. 3.

Appendix III.—References

1. Aneja, I., and Roll, F., "An Experimental and Analytical Investigation of a Horizontally Curved Box-Beam Highway Bridge Model," *American Concrete Institute Special Publication SP-26*, 1971, pp. 379-410.
2. Ashwell, D. G., and Sabir, A. B., "Limitations of Certain Curved Finite Elements when Applied to Arches," *International Journal of Mechanical Sciences*, Vol. 13, 1971, pp. 133-139.
3. Bažant, Z. P., "Pièces longues a voiles épais et calcul des poutres a section déformable," *Annales des Ponts et Chaussées*, No. III, 1969, pp. 115-169; also *Stavebnícky Časopis SAV*, Vol. 15, 1967, pp. 541-555.
4. Bažant, Z. P., "A Correlation Study of Formulations of Incremental Deformation and Stability of Continuous Bodies," *Transactions*, American Society of Mechanical Engineers, *Journal of Applied Mechanics* Vol. 38, 1971, pp. 919-928.
5. Bažant, Z. P., and El Nimeiri, M., "Large Deflection Spatial Buckling of Thin-Walled Beams and Frames," *Journal of the Engineering Mechanics Division*, ASCE, Vol. 99, No. EM6, Proc. Paper 10247, Dec., 1973, pp. 1259-1281.
6. Benscoter, S. U., "A Theory of Torsion Bending for Multicell Beams," *Journal of Applied Mechanics, Transactions*, American Society of Mechanical Engineers, Vol. 76, 1954, pp. 25-34.
7. Buragohain, D. N., and Babu, L. A., "Analysis of Curved Box Girder Bridges," *Journal of the Structural Division*, ASCE, Vol. 99, No. ST5, Proc. Paper 9715, May, 1973, pp. 799-819.
8. Cheung, M. S., and Cheung, Y. K., "Analysis of Curved Box Girder Bridges by Finite Strip Method," *Publications*, International Association for Bridge and Structural Engineering, Vol. 31-I, 1971, pp. 1-20.

9. Cheung, Y. K., "Analysis of Box Girder Bridges by the Finite Strip Method," *American Concrete Institute Special Publication SP-26*, 1971, pp. 357-378.
10. Dabrowski, R., "Der Schubverformungseinfluss auf die Wölbkrafttorsion der Kastenträger mit verformbarem biegesteifem Querschnitt," *Der Bauingenieur*, 1965, p. 445; (also 7th Congress, International Association for Bridge and Structural Engineering, Rio de Janeiro, Brazil, 1964, p. 299.
11. De Fries-Skene, A., and Scordelis, A. C., "Direct Stiffness Solution for Folded Plates," *Journal of the Structural Division*, ASCE, Vol. 90, No. ST4, Proc. Paper 3994, Aug., 1964, pp. 15-47.
12. Goldberg, J. E., and Leve, H. L., "Theory of Prismatic Folded Plate Structures," *Publications*, International Association for Bridge and Structural Engineering, Vol. 17, 1957, pp. 59-86.
13. Křístek, V., "Tapered Box Girders of Deformable Cross Section," *Journal of the Structural Division*, ASCE, Vol. 96, No. ST8, Proc. Paper 7489, Aug., 1970, pp. 1761-1793.
14. Lim, P. T. K., Kilford, J. K., and Moffatt, K. R., "Finite Element Analysis of Curved Box Girder Bridges," *Developments in Bridge Design and Construction*, University College, Cardiff, Wales, Crosby, Lockwood and Son, London, England, 1971.
15. Loo, Y-C., and Cusens, A. R., "Developments of the Finite Strip Method in the Analysis of Cellular Bridge Decks," *Developments in Bridge Design and Construction*, University College, Cardiff, Wales, Crosby, Lockwood and Son, London, England, 1971.
16. Megard, G., "Planar and Curved Shell Elements," *Finite Element Methods in Stress Analysis*, I. Holand and K. Bell, eds., Tapir-Technical University, Trondheim, Norway, 1970, pp. 287-318.
17. Meyer, C., and Scordelis, A. C., "Computer Program for Prismatic Folded Plates with Plate and Beam Elements," *Structural Engineering and Structural Mechanics, Report No. SESM70-8*, University of California, Berkeley, Calif., 1970.
18. Meyer, C., and Scordelis, A. C., "Analysis of Curved Folded Plate Structures," *Journal of the Structural Division*, ASCE, Vol. 97, ST10, Proc. Paper 8434, 1971, pp. 2459-2480.
19. Nowinski, J., "Theory of Thin-Walled Bars," *Applied Mechanics Reviews 12*, No. 4, 1959 (survey); up-dated in *Applied Mechanics Surveys*, M. N. Abramson, et al., eds., Spartan Books, Washington, 1966, pp. 325-338.
20. Oden, T., *Finite Elements of Nonlinear Continua*, John Wiley, and Sons, Inc., New York, N.Y., 1971.
21. Przemieniecki, J. S., *Theory of Matrix Structural Analysis*, McGraw-Hill Book Co., Inc., New York, N.Y., 1968.
22. Sabir, A. B., and Ashwell, D. G., "A Comparison of Curved Beam Finite Elements when Used in Vibration Problems," *Journal of Sound and Vibration*, Vol. 18, 1971, pp. 555-563.
23. Scordelis, A. C., "Analytical Solutions for Box Girder Bridges," *Developments in Bridge Design and Construction*, University College, Cardiff, Wales, Crosby, Lockwood and Son, London, England, 1971.
24. Scordelis, A. C., and Davis, R. E., "Stresses in Continuous Concrete Box Girder Bridges," *American Concrete Institute Special Publication SP-26*, 1971, pp. 357-378.
25. Sisodiya, R. G., and Cheung, Y. K., "A Higher Order In-plane Parallelogram Element and its Application to Skewed Curved Box-Girder Bridges," *Developments in Bridge Design and Construction*, University College, Cardiff, Wales, Crosby, Lockwood and Son, London, England, 1971.
26. Timoshenko, S. P., and Gere, J. M., *Theory of Elastic Stability*, 2nd ed., McGraw Hill Book Co., Inc., New York, N.Y., 1961, pp. 212-217.
27. Vlasov, V. Z., *Thin-Walled Elastic Bars* (in Russian) 2nd ed., Fizmatgiz, Moscow, U.S.S.R. 1959; also (in English), Israel Program for Scientific Translations, Jerusalem, Israel, 1961.
28. Zienkiewicz, O. C., *The Finite Element Method in Engineering Science*, McGraw-Hill Book Co., Ltd., London, England, 1971.
29. Zienkiewicz, O. C., Taylor, R. L., and Too, J. M., "Reduced Integration Techniques

in General Analysis of Plates and Shells," *International Journal for Numerical Methods in Engineering*, Vol. 3, 1971, pp. 255-290.

Appendix IV.—Notation

The following symbols are used in this paper:

A = area of cross section;
$\mathbf{A}$ = matrix of interpolation functions, Eq. 7;
a, b = width and depth of box (Fig. 1);
$\mathbf{a}_i, \mathbf{b}_i, a_{x_i}, a_{y_i}, \ldots b_{z_i}$ = basic vectors of end cross section i and their components;
$\mathbf{c}, \mathbf{c}_1, \mathbf{c}_2$ = matrices in Eq. 22 and Eq. 30;
$e_z, e_{zs}, \mathbf{e}$ = small incremental normal and shear strains and their column matrix, Eq. 11;
$\mathbf{J}, |J|$ = Jacobian matrix of coordinate transformation (Eq. 15) and its determinant;
$\mathbf{k}, \mathbf{K}, \mathbf{K}^1, \mathbf{K}^0$ = condensed and full stiffness matrix and its parts (Eqs. 19-23);
k_s, m_s = transverse incremental curvature and bending moment in wall;
l, L = length of element and length of beam;
M_x^0, P^0 = initial bending moment and axial force (Eq. 20);
P_k, Q_k = generalized cross section forces, Eq. 4;
p_z, p_s, p_n = components of distributed load, Eq. 8;
$\mathbf{q}, \mathbf{q}^b, \mathbf{q}^c$ = column matrix of element displacements (Eq. 6) and its parts referring to boundary nodes and center node;
s = coordinate along wall in cross section of beam;
u, v, w = displacements along beam and within cross section plane, tangential and normal to wall;
W, W_1, W_0 = virtual work and its components, Eqs. 8-10;
x, y, z = cartesian components of element;
δ = first variation;
$\delta_1, \delta_2, \delta$ = thickness of horizontal and vertical sides of box and at general point;
$\epsilon_{zs}, \gamma_{zs}$ = normal and shear components of finite incremental strain, Eq. 11;
ξ, η, ζ = cartesian coordinates of parent unit element;
ρ = distance of wall tangent from beam axis (Eq. 3);
$\sigma_z, \tau_{zs}, \underline{\sigma}$ = incremental normal and shear strains and their column matrix;
σ_z^0, τ_{zs}^0 = initial normal stresses, Eqs. 10 and 20; and
ϕ_k, ψ_k, χ_k = displacement distribution modes within cross section, Eq. 2.

Subscripts

i, j = ends of element.

Superscript

T = transpose of matrix.

10877 CURVED BOX GIRDERS AT INITIAL STRESS

KEY WORDS: Beams (supports); Bending; Box girders; Bridges (structures); Buckling; **Curved beams;** Finite element method; Stability; **Structural engineering;** Thin-wall structures; Torsion

ABSTRACT: A method of analysis of the global behavior of long curved or straight single-cell girders with or without initial stress is presented. It is based on thin-wall beam elements that include the modes of longitudinal warping and of transverse distortion of cross section. Deformations due to shear forces and transverse bimoment are included, and it is found that the well-known spurious shear stiffness in very slender beams is eliminated by virtue of the fact that the interpolation polynomials for transverse displacements and for longitudinal displacements (due to rotations and warping) are linear and quadratic, respectively, and an interior mode is used. The element is treated as a mapped image of one parent unit element and the stiffness matrix is in integration of in three dimensions, which is numerical in general, but could be carried out explicitly in special cases. Numerical examples of deformation of horizontally curved bridge girders, and of lateral buckling of box arches, as well as straight girders, validate the formulation and indicate good agreement with solutions by other methods.

REFERENCE: Bazant, Zdenek P., and El Nimeiri, Mahjoub, "Stiffness Method for Curved Box Girders at Initial Stress," *Journal of the Structural Division,* ASCE, Vol. 100, No. ST10, **Proc. Paper 10877,** October, 1974, pp. 2071-2090